Exploring Different Cationic Alkyl Side Chain Designs for Enhanced Alkaline Stability and Hydroxide Ion Conductivity of Anion-Exchange Membranes

ARTICLE *in* MACROMOLECULES · AUGUST 2015

Impact Factor: 5.8 · DOI: 10.1021/acs.macromol.5b01302

2 AUTHORS:

Hai-Son Dang
Lund University
7 PUBLICATIONS **37** CITATIONS
SEE PROFILE

Patric Jannasch
Lund University
108 PUBLICATIONS **2,515** CITATIONS
SEE PROFILE

Macromolecules

Article

pubs.acs.org/Macromolecules

Exploring Different Cationic Alkyl Side Chain Designs for Enhanced Alkaline Stability and Hydroxide Ion Conductivity of Anion-Exchange Membranes

Hai-Son Dang and Patric Jannasch*

Polymer & Materials Chemistry, Department of Chemistry, Lund University P.O. Box 124, SE-221 00, Lund, Sweden

Supporting Information

ABSTRACT: In order to systematically improve the performance of anion-exchange membranes (AEMs) for alkaline fuel cells, a series of poly(phenylene oxide)s (PPOs) was tethered with cationic alkyl side chains of different lengths and configurations. PPO was first functionalized with bromomethyl and longer bromoalkyl side chains, respectively, before introducing quaternary ammonium (QA) groups via Menshutkin reactions involving trimethylamine and dimethyloctylamine, respectively. This resulted in samples with QA groups attached to PPO either directly in benzylic positions, or via flexible pentyl and heptyl spacer units, respectively. In addition, the polymers were configured with or without octyl extender chains pendant to the QA groups. All the cationic PPOs had an excellent solubility in, e.g., methanol and dimethyl sulfoxide, and flexible and mechanically robust AEMs with an ion exchange capacity of ~1.4 mequiv g^{-1} were cast from solution. Analysis by small-angle X-ray scattering showed that the flexible spacer units greatly facilitated efficient ionic phase separation, regardless of the presence of the extender chain. These AEMs reach very high OH^- conductivities, exceeding 0.1 S cm^{-1} at 80 °C. A clear optimum conductivity was observed for the AEMs with pentyl spacers. Despite a markedly lower water uptake, AEMs configured with additional extender chains still reached a high conductivity, 0.07 S cm^{-1} at 80 °C. Importantly, the spacer units induced a high alkaline stability and no degradation of these AEMs was detected after storage in 1 M NaOH at 80 °C during 8 days. In comparison, the benchmark materials with QA groups placed in conventional benzylic positions severely degraded under the same conditions. The findings demonstrated that AEMs suitable for fuel cell applications can be achieved by tuning the configuration of flexible cationic alkyl side chains to reach an excellent combination of ionic phase separation, chemical stability, water uptake, and OH^- conductivity.

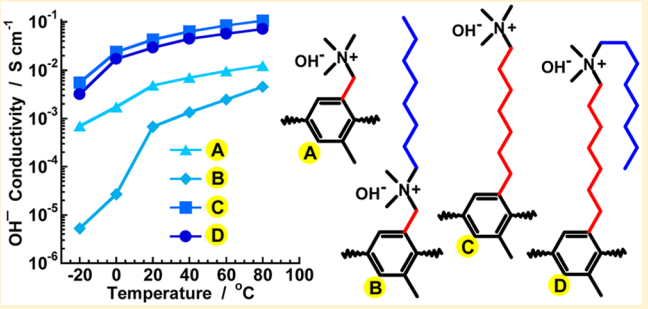

1. INTRODUCTION

Significant research efforts are currently invested in the molecular design, synthesis, and characterization of robust and highly anion-conducting polymers. These materials are currently investigated as electrolyte membranes for use in a range of emerging electrochemical energy conversion and storage devices including redox-flow batteries, reverse electrodialysis, metal-air batteries, and alkaline membrane fuel cells (AMFCs).[1,2] In particular, AMFCs are receiving increasing attention relative to proton-exchange membrane fuel cells because the alkaline operating conditions bring significant advantages in the form of faster oxygen reduction kinetics and improved fuel oxidation kinetics.[1,2] This may enable the use of nonprecious metal catalysts and lead to higher cell efficiencies to significantly reduce the cost of the fuel cell system. The anion-exchange membrane (AEM) is a critical component, since its OH^- conductivity and alkaline stability to a great extent determine the performance and lifetime of the AMFC system. Today, one of the main challenges in the commercialization of AMFCs is to develop membrane materials that are sufficiently mechanically and chemically stable while providing high OH^- conductivity at moderate water swelling.[1−7] Specifically, a high stability above 80 °C is desirable because the solubility of CO_2 in water is considerably reduced above this temperature to prevent the formation of bicarbonate/carbonate. Concurrently, the kinetics of the electrode reactions is enhanced. A wide range of polymers including aromatic polyethers, polysulfones, polyketones and polystyrenes have been functionalized with quaternary ammonium (QA) groups and investigated as AEM materials.[1−7] These polymers are typically prepared by chloromethylation of the aromatic backbones using chloromethyl methyl ether, followed by Menshutkin reactions with trimethylamine to introduce the QA groups. This route generally gives poor control of the concentration and location of the ionic groups, and requires handling of carcinogenic chloromethylation agents. Alternatively, QA groups may be introduced via benzyl bromide groups prepared through radical bromination of benzylic

Received: June 16, 2015
Revised: July 31, 2015
Published: August 11, 2015

DOI: 10.1021/acs.macromol.5b01302
Macromolecules 2015, 48, 5742−5751

methyl groups on the polymer backbone using, e.g., azobis(isobutyronitrile) and *N*-bromosuccinimide.[8−13] This normally provides improved precision in the concentration and placement of the QA groups in the polymer structure. Still, both these routes invariably result in QA groups placed on benzylic sites, in nearly all cases very close to the polymer backbone. This will restrict the local mobility of the QA groups and prevent the distinct phase separation which seems to be necessary to reach high anionic conductivity of AEMs. To facilitate phase separation, QA groups have been highly concentrated to specific units or segments in statistical[13,14] and block[15−20] copolymers, and to stiff side groups.[21] However, this strategy may lead to limitations in ion-dissociation caused by the close proximity of the cations in the polymer structure.[22]

Because of its high basicity and nucleophilicity, the hydroxide ion is prone to attack and degrade QA groups and other cationic moieties, as well as polymer backbones which are activated for hydrolysis under basic conditions. Several degradation pathways have been reported for QA groups including β-hydrogen Hofmann elimination, direct nucleophilic substitution at an α-carbon and via ylide formation.[1] QA groups in benzylic positions have proven to be especially sensitive toward degradation, and also seem to activate the cleavage of adjacent ether links in aromatic polymer backbones.[23] Several recent studies of low-molecular weight analogues suggest that QA groups substituted with long alkyl chains possess a significantly higher alkaline stability than benzyl-substituted cations.[24,25] However, attaching QA groups to suitable polymer backbones via long alkyl spacers is difficult to achieve and calls for new synthetic approaches. Hence only a few examples have yet been reported.[26−30] In an early study, Tomoi et al. reported on enhanced stability by placing a long alkyl spacer between polystyrene backbones and the QA groups.[26] Later, Hibbs functionalized a polyphenylene with QA groups via hexyl spacers and found a significant increase in the stability in comparison with that of a corresponding benzyltrimethylammonium functionalized polymer.[27] In a recent communication, we reported on the attachment of QA groups to poly(phenylene oxide) (PPO) via flexible and stable heptyl spacers by using a straightforward synthetic route involving bromoalkylation and quaternization.[28] AEMs based on these polymers showed a pronounced ionic phase separation, enhanced hydroxide ion conductivity and much improved alkaline stability in comparison to corresponding polymers with the QA groups conventionally located in benzylic positions on the PPO backbone. These encouraging findings have prompted us to further investigate and optimize the flexible spacer concept to tailor AEM properties for use in fuel cell applications.

In the present work we have attached different types of QA-containing alkyl side chains to PPO and studied their influence on the AEM properties. In particular, we have investigated the effect of different side chain configurations based on spacer units in-between the QA group and the polymer backbone, as well as on extender units pendant to the QA groups, as outlined in Scheme 1. In addition, our aim was to clarify the influence of the alkyl spacer length on the membrane properties. A series of six PPOs having different combinations of spacer units and extender chains, but similar ionic contents, were prepared by bromoalkylations and quaternizations. Subsequently, membranes were cast and a detailed characterization of ionic segregation, alkaline stability, water uptake and OH^- conductivity of the AEMs was performed to establish the relationships between side chain configuration, membrane morphology and the properties of these materials.

Scheme 1. Schematic Illustration of Polymer Backbones (in Black) Tethered with Cationic Side Chains Having the Different Combinations of Spacer Units (in Red) and Extender Chains (in Blue) Synthesized and Investigated in the Present Work

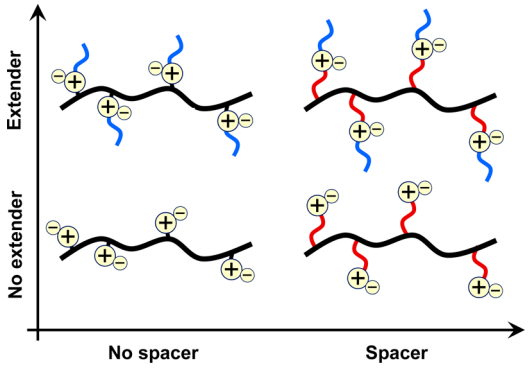

2. EXPERIMENTAL SECTION

Materials. Tetrahydrofuran (THF, HPLC grade, Honeywell) was dried over molecular sieves (Acros; 4 Å, 8−12 mesh) before use. Poly(2,6-dimethyl-1,4-phenylene oxide) (PPO, Sigma-Aldrich, M_n = 20 kg mol^{-1}, $M_wM_n^{-1}$ = 2.3), *n*-butyllithium (*n*-BuLi, 2.5M, solution in hexanes, Acros), 1,6-dibromohexane (98%, Acros), NBS (99%, Acros), azobis(isobutyronitrile) (AIBN, 98%, Acros), chlorobenzene (99+%, Fluka Analytical), *N*-methyl-2-pyrrolidone (NMP, reagent grade, Acros), trimethyl amine (TMA, 7.3 M aq. solution, Acros), *N*,*N*-dimethyloctylamine (DMOA, 97%, Acros), 1,4-dibromobutane (99%, Sigma-Aldrich), diethyl ether (99+%, Sigma-Aldrich), silver nitrate (99,995%, Sigma-Aldrich), methanol (MeOH, HPLC grade, Honeywell), 1,2-dichlorobenzene (99+%, Fluka Analytical), and 2-propanol (IPA, HPLC grade, Honeywell) were used as received.

Polymer Synthesis. A series of six PPO samples with different combinations of alkyl spacer units and extender chains, but with similar ionic contents, were prepared via quaternization of bromoalkylated and benzyl brominated samples (Scheme 2). The samples were designated as PPO-*n*Q*m* where *n* and *m* are the number of carbon atoms in the spacer and extender chain, respectively.

PPO was bromoalkylated by lithiation and reaction with either 1,4-dibromobutane or 1,6-dibromohexane to prepare polymers with a degree of bromination of 22 and 24%, respectively (DB, percentage of bromoalkylated benzylic methyl groups of the PPO). The samples were designated as PPO-*n*Br where *n* was the number of carbon atoms in the bromoalkyl chain, in the present case *n* = 5 and 7, respectively. Here, the synthesis of PPO-5Br will serve as an example. A 4-neck 500 mL round bottomed flask equipped with a magnetic stirrer and fitted with thermometer, a rubber septum and an argon inlet−outlet was charged with PPO (3 g, 24.97 mmol repeat units) and dry THF (300 mL). The mixture was degassed and stirred at 55 °C until a homogeneous solution was formed. After allowing the solution to cool to room temperature, the reactor system was repeatedly degassed with argon using at least seven evacuation cycles. Remaining traces of impurities were titrated by addition of a few droplets of *n*-BuLi solution until a light yellow color persisted to indicate the beginning of the polymer lithiation reaction. Next, 15 mL *n*-BuLi solution (37.50 mmol) was added dropwise and the reaction mixture was kept during 3 h under stirring. At this time, the lithiated PPO had formed a fine precipitate. Consequently, the mixture was heated to 50 °C until all the polymer completely redissolved to form a red homogeneous solution. The polymer solution was cooled to −78 °C using a dry ice/IPA bath, followed by an instantaneous addition of a 200% molar excess of 1,4-dibromobutane (13.6 mL, 112.5 mmol) to quench the lithiated sites on the PPO. A light yellow solution was immediately

DOI: 10.1021/acs.macromol.5b01302
Macromolecules 2015, 48, 5742−5751

Scheme 2. Synthetic Pathways to PPO Carrying QA Groups Placed on Side Chains with Different Spacer Lengths (n = 5 or 7), with and without Extender Chains (PPO-nQ8 and PPO-nQ1, Respectively)[a]

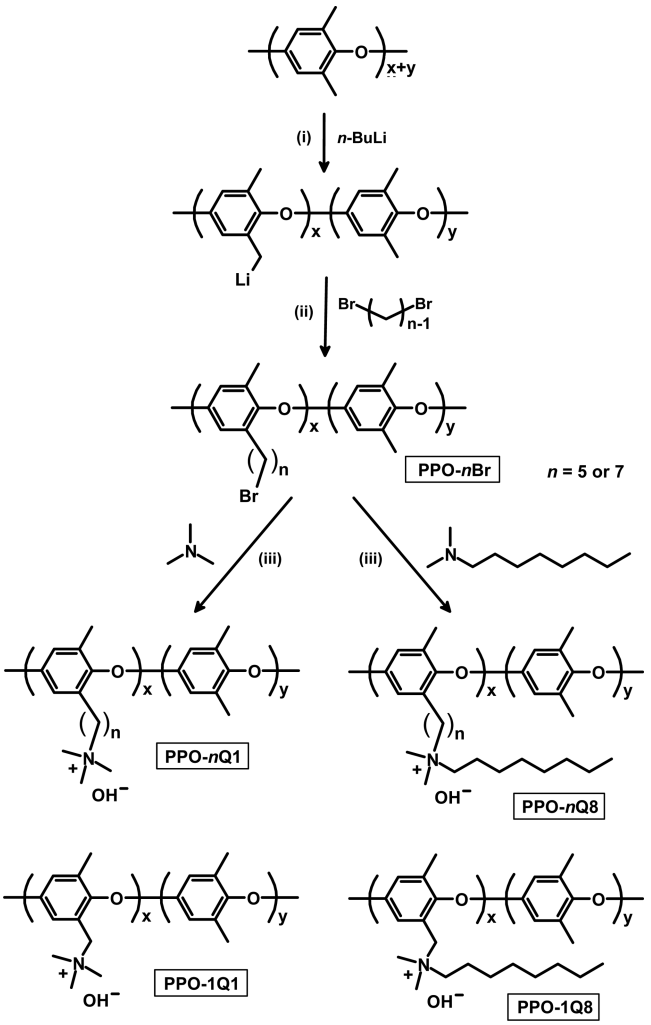

[a]Key (i) THF, −78 °C, (ii) THF, −78 °C, (iii) NMP, 25 °C; aqueous. NaOH, 25 °]. Corresponding PPOs functionalized with QA groups in benzylic positions (PPO-1Q8 and PPO-1Q1) were prepared via benzylic bromination and reaction with the respective trialkylamine. The IEC values for all the PPO-nQm samples were kept in a narrow range between 1.3 and 1.5 mequiv g^{-1}.

formed which was kept under stirring overnight while allowed to reach room temperature. After passage through a glass filter (porosity 2), the solution was added dropwise to methanol to precipitate the product as a white powder. The product was collected by filtration, washed repeatedly with fresh methanol and dried at 50 °C over 2 days.

PPO was benzyl brominated to prepare sample PPO-1Br with DB = 21% by following a previously described method.[28] PPO (10.0 g, 83.23 mmol repeat units) was dissolved in 200 mL 1,2-dichlorobenzene in a 2-neck bottomed flask equipped with a reflux condenser under nitrogen atmosphere. The colorless solution was first degassed by bubbling of nitrogen gas, followed by addition of NBS (4.47 g) and AIBN (0.265 g). The reaction was then allowed to proceed for 4 h at 110 °C after which the solution was poured into IPA to precipitate the product. The benzyl brominated polymer was finally washed in IPA and water and dried *in vacuo* at 50 °C during 24 h.

The cationic side chains of the six PPO-nQm samples were prepared via Menshutkin reactions in which the bromine atoms of the benzyl brominated (n = 1) and bromoalkylated (n = 5 and 7) polymers were displaced by TMA (m = 1) and DMOA (m = 8), respectively, to form the QA groups. After preparing solutions containing 5 wt % of the respective polymers in NMP, a 1000% molar excess of TMA and DMOA, respectively, was added. The homogeneous solutions were kept under stirring in a sealed vessel at room temperature for at least 4 days to achieve full conversion. The yellow solutions were added dropwise to diethyl ether to precipitate the products as white powders. After filtration and washing twice with diethyl ether, the white precipitates were dried at room temperature for 2 days under vacuum before obtaining the cationic polymers in the ammonium bromide form.

Structural Characterization. ^{1}H NMR spectra were obtained with a Bruker DR X400 spectrometer at 400.13 MHz using $CDCl_3$ (δ = 7.26 ppm) or DMSO-d_6 (δ = 2.50 ppm) solutions of the samples. A size-exclusion chromatograph equipped with a series of three Shodex gel colums (KF-805, -804, and -802.5) and a refractive index detector was used for the determination of M_n and M_w of the native and brominated PPO. Polystyrene standards with low polydispersity were used to calibrate the SEC data (M_n = 650 kg mol^{-1} from Water Associates, and M_n = 96 and 30 kg mol^{-1} from Polymer Laboratories, and M_n = 3.18 kg mol^{-1} from Agilent Technologies). All samples were first dissolved in chloroform and then passed through a Teflon filter with the pore size 0.45 μm before SEC analysis at room temperature at a chloroform elution rate of 1 mL min^{-1}.

Membrane Preparation. AEMs were prepared from all the PPO-nQm samples in the ammonium bromide salt form. An amount of 0.15 g of the polymer was dissolved in NMP (3 g) and poured onto a glass Petri dish with a 5 cm diameter. The membranes were cast in an oven at 80 °C during 36 h. The resulting films were peeled from the dish and thoroughly washed with deionized water. Finally, the membranes were stored in deionized water during at least 48 h at room temperature prior to analysis. The average membrane thickness was approximately 60 μm.

Thermal Characterization. A TA Instruments thermogravimetric analyzer (TGA Q500) was employed to study the thermal decomposition of the AEM samples. The samples were first dried in a vacuum oven at 50 °C until constant weight. Prior to measurement, all samples were preheated during 10 min at 150 °C to remove traces of water. Data was then recorded at a constant heating rate of 10 °C min^{-1} in the temperature range 50−600 °C under nitrogen atmosphere. The decomposition temperature ($T_{d,95}$) was determined at 5% weight loss. Differential scanning calorimetry was performed to determine the glass transition temperature (T_g) using a DSC Q2000 analyzer from TA Instruments. DSC heating/cooling/heating data was recorded between 50 and 280 °C and T_g was determined from the second heating cycle.

Determination of Ion Exchange Capacity and Water Uptake. The ion exchange capacity (IEC) of the AEMs in the bromide salt form was determined by Mohr titrations. Membrane samples were dried in a vacuum oven at 50 °C at least 48 h and weighted before immersion in 0.2 M $NaNO_3$ (25.00 mL) during more than 48 h to achieve full ion exchange. The titration of the Br^- was carried out with 0.01 M aqueous $AgNO_3$ using potassium chromate (K_2CrO_4) as indicator.

All AEMs in the Br^- form were dried in a vacuum oven at 50 °C during at least 48 h and weighted to obtain the dry weight (W_{Br^-}). The dry membranes were then immersed in 1 M degassed aqueous NaOH solution in a desiccator for 48 h under nitrogen flow. Next, the samples were immersed in a beaker containing 1 M aq. NaOH under a protective blanket of nitrogen during 48 h. The membranes were then quickly transferred to a beaker containing degassed deionized water and washed for a few seconds. This process was repeated until the pH of the immersing water reached a value of 7. The membranes were then immersed in deionized water at least 24 h at room temperature in a nitrogen atmosphere. After equilibration in water, the membrane surfaces were quickly wiped dry with tissue paper and the weight of the wet membranes in hydroxide form (W'_{OH^-}) was determined. The dry weight of quaternized membranes in OH^- form (W_{OH^-}) was precisely calculated using IEC titration results and W_{Br^-}. The water uptake (WU) was then calculated as

DOI: 10.1021/acs.macromol.5b01302
Macromolecules 2015, 48, 5742−5751

$$\mathrm{WU} = \frac{W'_{OH^-} - W_{OH^-}}{W_{OH^-}} \times 100\% \quad (1)$$

Using the same procedure, water uptake measurements were carried out at temperatures of 40, 60, and 80 °C. The hydration number (λ), defined as the number of water molecules per QA group, was calculated as

$$\lambda = \frac{1000 \times (W'_{OH^-} - W_{OH^-})}{\mathrm{IEC} \times W_{OH^-} \times 18} \quad (2)$$

Conductivity Measurements. The hydroxide ion conductivity of the AEMs under fully hydrated conditions was measured using a Novocontrol high resolution dielectric analyzer 1.01 S at 50 mV over the frequency range 10^{-1} to 10^{7} Hz. The membranes in Br^- form were first ion exchanged to the OH^- form by immersion in 1 M NaOH for at least 48 h in a desiccator under a nitrogen atmosphere. After that, the membranes were repeatedly washed with degassed distilled water until the pH of washing water became neutral (pH ≈ 7). Finally, the membranes were mounted in a sealed two-probe cell for through-plane measurements under fully immersed conditions between −20 and +80 °C.

Small Angle X-ray Scattering. Small-angle X-ray scattering (SAXS) measurements were employed to characterize the morphology of dry AEMs in the Br^- form. The measurements were performed using a SAXSLAB ApS system (JJ-Xray, Denmark) combined with a Pilatus detector. The scattering vector (q) was calculated as

$$q = \frac{4\pi}{l[\sin 2\theta]} \quad (3)$$

where l is the wavelength of the Cu K(α) radiation (1.542 Å) and 2θ is the scattering angle. The average distance between ionic clusters (d) in the AEMs was calculated as

$$d = \frac{2\pi}{q} \quad (4)$$

Evaluation of Alkaline Stability. The chemical stability of the AEMs under alkaline conditions was studied by using ^{1}H NMR spectroscopy. Pieces of the membranes were stored in a sealed vessel containing 1 M aqueous NaOH at 80 °C using a temperature-controlled silicone oil bath. After 4 and 8 days of immersion, samples were taken out and washed with deionized water, before being soaked in 1 M aqueous NaBr at 50 °C for 48 h to obtain the Br^- salt form of the membrane pieces. In order to remove all excess NaBr, the samples were immersed in deionized water during 24 h and followed by extensive washing. All the samples were then dried at 50 °C for 24 h before dissolution in DMSO-d_6 under gentle heating and analysis by ^{1}H NMR spectroscopy as described above.

3. RESULTS AND DISCUSSION

Polymer Synthesis and Characterization. PPO is a high-performance aromatic polymer with excellent mechanical properties, and high chemical and thermal stability, making it suitable for preparation of membrane materials.[31] In particular, the PPO backbone contains no electron-withdrawing groups or links that activate the ether links for cleavage through nucleophilic attack by hydroxide ions. A high stability under alkaline conditions, combined with good film-forming properties, make PPO suitable for modification to produce AEMs for AMFC. Using different synthetic strategies, PPO can be modified in a variety of ways in either the aromatic or benzylic positions.[31,32]

In the present work PPO was bromoalkylated via benzylic lithiation and subsequent reaction with an α,ω-dibromoalkane, as we have reported previously (Scheme 2). Notably, organolithium chemistry is widely used industrially to, e.g., produce large volumes of polydiene rubbers and polystyrene-based thermoplastic elastomers.[33] In the present case, native PPO was lithiated in THF using *n*-butyllithium (*n*-BuLi) under argon at −70 °C. Under these conditions both aryl and benzyl positions are lithiated, but only the latter are sufficiently nucleophilic to displace the bromine atoms of bromoalkanes.[34−36] Approximately 3 h after adding *n*-BuLi, an excess of either 1,4-dibromobutane or 1,6-dibromohexane was quickly added to immediately quench all the benzyl lithiated sites, leading to the formation of bromopentyl or bromoheptyl side chains, respectively, on the PPO backbone (Scheme 1). The momentaneous quenching of all the lithiated sites was essential to effectively depress cross-linking reactions which may otherwise occur due to of the difunctionality of the dibromoalkanes.

By following this procedure, two PPO samples were bromoalkylated with good precision to contain approximately the same concentration of bromopentyl and bromoheptyl side chains, respectively (Table 1). The degree of bromination of these samples, designated PPO-5Br and PPO-7Br, respectively, was controlled to target AEMs with IEC values of 1.3−1.5 mequiv g^{-1} depending on side chain configuration. A comparison of the ^{1}H NMR spectra of the native PPO and sample PPO-5Br in Figure 1a and b, respectiviely, confirmed the successful bromoalkylation (additional NMR spectra available as Supporting Information, Figure S1). A new signal (c) appeared at 3.4 ppm from the $-CH_2Br$ protons and a band of signals from additional methylene protons was seen in the range 1.2−2.0 ppm. The values of DB were calculated by comparing the integrated signals c and b, the latter centered at 6.5 ppm and originating from the aromatic PPO protons (Figure 1b). The M_n values and the polydispersity ($M_wM_n^{-1}$) were found by SEC to increase after the bromoalkylation, which may indicate some polymer coupling reactions (Table 1). However, no gel formation was noticed in any of the modified polymers. As expected, the glass transition temperature decreased considerably, from T_g = 232 °C for native PPO to approximately 160 °C for the two bromoalkylated samples, because of the internal plasticization caused by the flexible alkyl side chains (Table 1, DSC traces in Supporting Information, Figure S2).

Table 1. Molecular Weight and Thermal Data of Native and Brominated PPO

sample	M_n [kg mol^{-1}] [a]	$M_wM_n^{-1}$ [kg mol^{-1}] [a]	DB [%]	T_g [°C]	$T_{d,95}$ [°C] [b]
PPO	20	2.3	0	232	419
PPO-1Br	22	4.1	21	231	289
PPO-5Br	22	2.4	22	161	336
PPO-7Br	26	4.0	24	158	345

[a]Examined by SEC using PS standards. [b]Measured by TGA under N_2.

In addition to the bromoalkylations, PPO was benzyl brominated in order to introduce QA groups placed directly on the methyl groups on the backbone. The bromination was carried out via radical-mediated benzylbromination using *N*-bromosuccinimide and azobis(isobutyronitrile), as reported previously,[28] and was targeted to reach the same level of bromination as PPO-5Br and PPO-7Br. The T_g of the benzylbrominated sample (PPO-1Br) was found very close to that of the native PPO. As seen in Table 1, the thermal decomposition temperature, $T_{d,95}$, decreased with 130 °C after

DOI: 10.1021/acs.macromol.5b01302
Macromolecules 2015, 48, 5742−5751

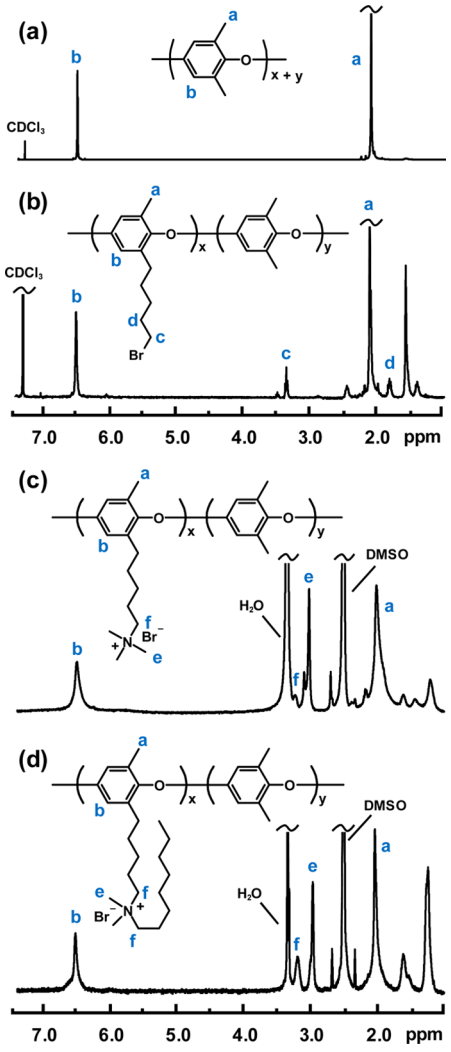

Figure 1. ^{1}H NMR spectra of native PPO (a), the bromoalkylated precursor PPO-5Br (b) and the quaternized samples PPO-5Q1 with a spacer unit (c), and PPO-5Q8 with both a spacer and an extender unit (d).

the benzylic bromination. As expected, the $T_{d,95}$ value decreased far less after the bromoalkylations, 83 and 74 °C, respectively.

All the brominated polymers were quaternized in Menshutkin reactions by which the bromine atoms were efficiently displaced by either trimethylamine or octyldimethylamine to form six PPO-*n*Q*m* samples with approximately the same cationic content, but with different QA side chain configurations, i.e. n = 1, 5, or 7 carbon atoms and m = 1 or 8 carbon atoms. (Scheme 1). In all cases, ^{1}H NMR analysis showed signals from the methylene and the methyl protons of the QA groups at 3.25 and 3.0 ppm, respectively (Figure 1, parts c and d). Further shifts from the additional methylene protons of the side chains appeared between 1.0 and 1.75 ppm. Mohr titrations of the Br^- content confirmed full quaternization in agreement with the DB values of the respective brominated precursor polymers, and corresponded to IEC values between 1.3 and 1.5 mequiv g^{-1} (Table 2). The PPO-*n*Q*m* samples were all soluble in methanol, DMSO and NMP, but remained insoluble in water up to at least 80 °C (see Supporting Information, Table S1). This suggests that these ionomers can be employed in the fabrication of catalyst layers for use in AMFCs.

Membrane Morphology. Flexible, transparent and mechanically stable AEMs with approximately the same ionic concentration and a thickness of ~60 μm were cast from NMP solutions of the PPO-*n*Q*m* samples at 80 °C (Table 2). Dry membranes in the Br^- form were investigated by small-angle X-ray scattering (SAXS) to study their morphology and ability to form ionic clusters. In general, the characteristic separation distance (d) between the ion-rich domains in ion-containing polymers can be observed via the value of q at the scattering maximum (q_{max}) provided by the so-called ionomer peak.[37] As seen in Figure 2, the membrane without any spacer or extender

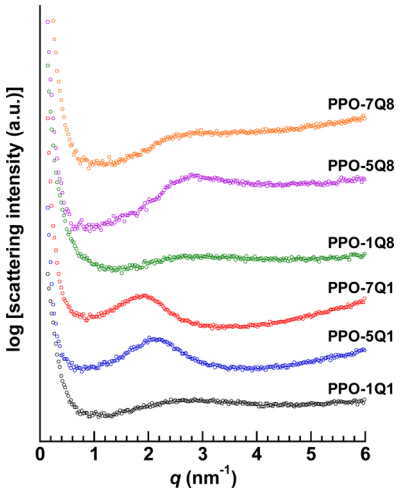

Figure 2. SAXS profiles of AEMs in the Br^- form based on PPO-*n*Q*m* samples functionalized with side chains having different combinations of spacer and extender chain lengths in the narrow IEC range between 1.3 and 1.5 mequiv g^{-1}. The data have been shifted vertically for clarity.

chains (PPO-1Q1) showed only a very weak ionomer peak at q_{max} ~ 2.8 nm^{-1}, corresponding to a characteristic distance of d

Table 2. Properties of the AEM Based on the QA Functional PPOs

AEM	IEC_{NMR} [a] [mequiv g^{-1}]	IEC_{titr} [a] [mequiv g^{-1}]	$T_{d,95}$ [b] [°C]	q_{max} [c] [nm^{-1}]	d [c] [nm]	WU_{20} [d] [wt %]	λ_{OH^-} [d]
PPO-1Q1	1.5 (1.4)	1.5 (1.4)	199	2.8	2.2	20	7
PPO-1Q8	1.3 (1.2)	1.4 (1.3)	188	2.8	2.2	9	4
PPO-5Q1	1.5 (1.4)	1.5 (1.4)	214	2.0	3.1	39	14
PPO-5Q8	1.3 (1.2)	1.4 (1.3)	206	3.0	2.1	19	8
PPO-7Q1	1.5 (1.4)	1.5 (1.4)	213	1.8	3.6	30	11
PPO-7Q8	1.3 (1.2)	1.3 (1.2)	205	2.8	2.2	16	7

[a]IEC for the OH^- form (values within parentheses are for the Br^- form). [b]Measured by TGA under N_2. [c]Measured by SAXS in the dry Br^- form. [d]Immersed in OH^- form at 20 °C.

DOI: 10.1021/acs.macromol.5b01302
Macromolecules 2015, 48, 5742−5751

~ 2.2 nm. This indicated very poor cluster formation and a low level of organization of the QA groups. When the distance between the PPO backbone and the QA groups was increased by adding a flexible spacer (PPO-5Q1 and PPO-7Q1), the SAXS profiles showed clear ionomer peaks at q_{max} = 2.0 and 1.8 nm^{-1}, respectively. These values correspond to characteristic distances of d = 3.1 and 3.6 nm, respectively, and showed that the introduction of the spacer units greatly facilitated the formation of distinct ionic clusters in the AEMs. As expected, the longer spacer unit resulted in a longer separation distance in the membrane and d increased linearly with n, as seen in Figure 3. The absence of any second order peaks in the scattering

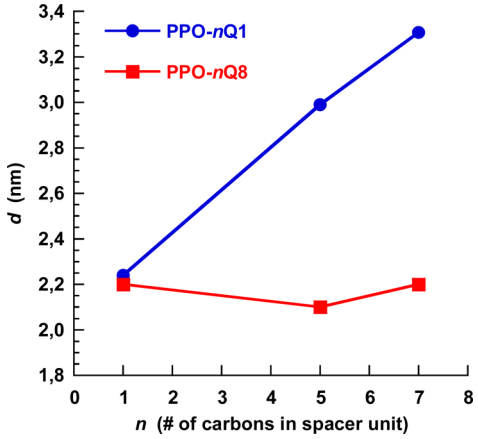

Figure 3. Variation of the d-spacing with the length (n) of the spacer unit for AEMs based on the PPO-nQ1 and PPO-nQ8 series.

profiles of the latter two membranes indicated that the ionic clusters were organized in the short-range, but without long-range order.

When an extender chain was added to QA groups placed directly on the backbone (PPO-1Q8), the SAXS profile was virtually identical to that of PPO-1Q1. Thus, a very weak ionomer peak indicated poor ionic clustering. Li et al. found similar SAXS patterns when studying benzyl-quaternized PPOs with hexyl and decyl extender chains.[38] When a spacer unit was inserted in addition to the extender chain, SAXS analysis again showed clear ionomer peak in the case of PPO-5Q8. A somewhat weaker scattering maximum was displayed by PPO-7Q8 (Figure 2). Perhaps in the latter case, the very long alkyl side chain, containing 16 atoms, partly hindered the ionic clustering process. The positions of the ionomer peaks for PPO-5Q8 and PPO-7Q8 were found at q_{max} = 3.0 and 2.8 nm^{-1}, respectively, corresponding to characteristic distances of d = 2.1 and 2.2 nm, respectively. Thus, the d-spacing measured for the membranes based on the polymers with both spacer and extender were considerably smaller (2.1−2.2 nm) than that measured for the membranes based on the polymers with only a spacer (3.1−3.6 nm). In addition, the d-spacing of the former membranes did not change significantly with n (Figure 3). This may indicate a different morphology with smaller scattering domains induced by the extender chains.

These results demonstrated that the ionic clustering is strongly facilitated by the presence of the spacer units which seemingy provide the QA groups with the necessary local mobility to efficiently phase separate from the polymer backbone. Notably, the addition of an extender chain reduced the length-scale of the phase separation. Still, the result on sample PPO-7Q8 hints that the ionic clustering may be impeded if the overall alkyl side chain (spacer + extender) becomes too long. In particular, the findings show that the spacer concept promoted a much more efficient phase separation of the ionic groups than that found in the PPO-1Q1 and PPO-1Q8 AEMs with the QA groups placed conventionally directly on the polymer backbone.

We have previously studied AEMs based on polysulfones with high local densities of QA groups to enhance ionic clustering and ion conductivity. Consequently, precisely two, three, or four QA[13] or imidazolium[39] groups were located in benzylic positions on single phenylene rings along the backbone. Although SAXS results show that the ions clustered efficiently to form distinct percolating hydrophilic phase domains, the gain in anionic conductivity was severly reduced by limitations in the ion dissociation caused by the very close proximity of the cationic sites in the polymer structure.[22] Hence, placing the QA groups on flexible alkyl spacers seems like a more efficient synthetic strategy to reach high conductivity.

Water Uptake and OH^- Conductivity. The water in the AEMs facilitates ion dissociation and is needed to form a percolating hydrated phase domain which is critical for the transport of the anions. It is however necessary to reach a balanced water uptake since too much water will lead to a high degree of swelling and hence compromised mechanical properties of the membranes.

Figure 4 shows the temperature dependence of the water uptake of the AEMs in the OH^- form when completely

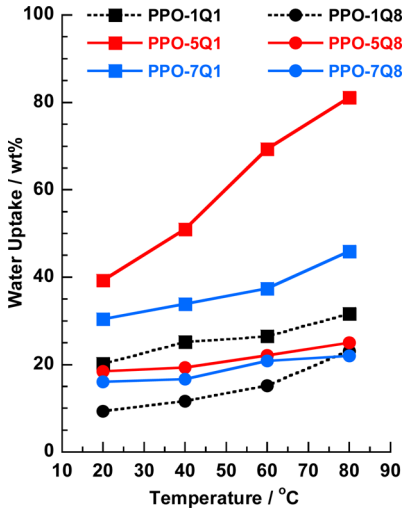

Figure 4. Water uptake of the fully hydrated (immersed) AEMs in the OH^- form as a function of temperature.

immersed in water between 20 and 80 °C. As expected, the water uptake increased with temperature. Although the ionic content of the present AEMs was very similar, the water uptake depended strongly on the different QA side chain configurations. It was clearly observed that the AEMs based on polymers with alkyl extender chains had a lower water uptake than those without. This may be because the former polymers form a morphology that accommodated lower water concentrations, or simply that the AEMs became more hydrophobic after the addition of the alkyl extender chains. Consistently, the AEMs with the QA groups placed on pentyl spacers took up most water, while those having the QA groups directly on the

DOI: 10.1021/acs.macromol.5b01302
Macromolecules 2015, 48, 5742−5751

PPO backbone took up the least. Thus, the presence of a spacer unit between the PPO backbone and the QA groups promoted ionic clustering and thus the formation of distinct water-filled domains.[28] However, it is plausible that if the spacer unit becomes too long the increased hydrophobicity induced by the alkyl chain may decrease the water uptake. All the membranes show a moderate water uptake, perhaps with the exception of PPO-5Q1 which reached 80 wt % at 80 °C. This is reflected in the highest λ-value of the AEMs, 14 at 20 °C (Table 2).

The OH^- conductivity under fully hydrated conditions was measured through the plane of the AEMs by electrochemical impedance spectroscopy (EIS) using a two probe cell fully flooded with deionized water. The data measured during heating from −20 to 80 °C is shown in Figure 5. In the range

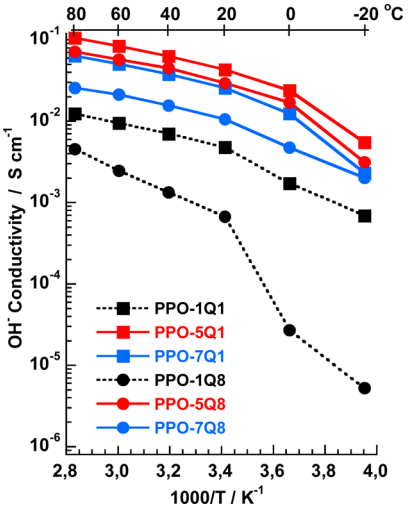

Figure 5. Arrhenius plots of the OH^- conductivity data measured by EIS of the PPO-*n*Q*m* AEMs under fully hydrated (immersed) conditions.

between −20 and +20 °C the conductivity increased more markedly for some AEMs because of the melting of frozen water in the membranes. Three of the membranes, PPO-5Q1, PPO-5Q8, and PPO-7Q1, reached very high conductivities, between 0.06 and 0.1 S cm^{-1} at 80 °C. Generally, conductivities of ca. 0.1 S cm^{-1} are needed for high current density cell outputs, while the operation of cells with AEMs having a conductivity of 0.05 S cm^{-1} is regarded as still quite reasonable.[1] As seen in Figure 5, the two AEMs with pentyl spacer units showed the highest conductivities, followed by the AEMs with heptyl spacers. The two membranes with the QA groups in benzylic positions thus showed the lowest levels of conductivity, almost an order of magnitude lower than the materials with pentyl spacers. The comparatively low conductivity of the latter two AEMs may be linked to their poor ion cluster formation, as indicated by SAXS, and their lower water uptake. As seen in Figure 5, the conductivity of all the membranes showed a similar apparent activation energy above 20 °C, except membrane PPO-1Q8 which showed a markedly higher value. This may be due to the development of a percolating conductive channel system as the water content of this membrane increased with temperature. Without doubt, the AEMs based on the polymers with spacer units evidently showed greatly enhanced OH^- conductivity in comparison to the membranes containing polymers with the QA groups attached directly to the backbone, at least partly because of a more localized conducting phase domain. The observed effect of the spacer units is in good agreement with our previously reported results on proton conducting sulfonated aromatic polymers. Placing the sulfonic acid groups on short alkyl[40] as well as aromatic[41,42] side chains greatly facilitated the ionic clustering, and the proton conductivity showed a trend of increasing values with the length and the sulfonic acid functionality of the side chain.[42] A further observation in the current study was that the presence of extender chains decreased the conductivity (Figure 5). This was at least partly a consequence of the reduced water uptake of these membranes in relation to that of the AEMs without extenders, as discussed above. Figure 6 shows the water uptake and the OH^-

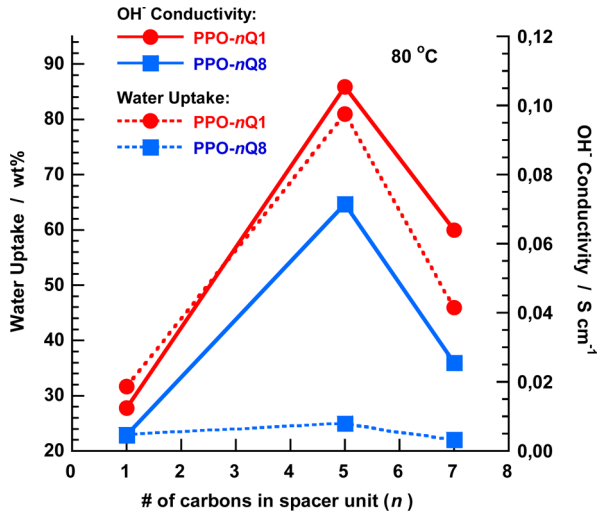

Figure 6. Water uptake and OH^- conductivity as a function of the length (n) of the spacer unit for AEMs based on the PPO-*n*Q1 and PPO-*n*Q8 series (IEC = 1.3−1.5 mequiv g^{-1}). Data measured at 80 °C with the membranes fully hydrated (immersed).

conductivity at 80 °C plotted against the spacer length. The data shows a clear optimum in both these properties at an alkyl spacer length somewhere between n = 1 and 5 carbons, most probably close to 5. This was regardless of the presence of an extender chain on the QA group. In addition, it is seen that the conductivity clearly followed the water uptake.

Figure 7, with the OH^- conductivity is plotted versus the water content, again shows the higher conductivity of the AEMs with spacer units at a given water content, as compared with the membranes without spacers. This demonstrates that the water in the former materials was used more efficiently to facilitate ion conductivity than that in the latter membranes. The data also illustrates the more restricted water uptake of the materials with extender chains. The higher conductivity of the materials without extender chains was achieved only at significantly higher water contents, especially when comparing the data of PPO-5Q1 and PPO-5Q8. At 20 and 80 °C, membrane PPO-5Q1 showed a conductivity of 0.043 and 0.11 S cm^{-1} at a water uptake of 39 and 81 wt %, respectively. However, the most efficient OH^- conductive AEM was probably membrane PPO-5Q8 which reached 0.03 and 0.07 S cm^{-1} at 20 and 80 °C, respectively. At these temperatures the water uptake of PPO-5Q8 was moderate at 18 and 25 wt %, respectively. As seen in Figure 7, the conductivity of PPO-5Q8 still increased significantly with the water uptake and it is likely

DOI: 10.1021/acs.macromol.5b01302
Macromolecules 2015, 48, 5742−5751

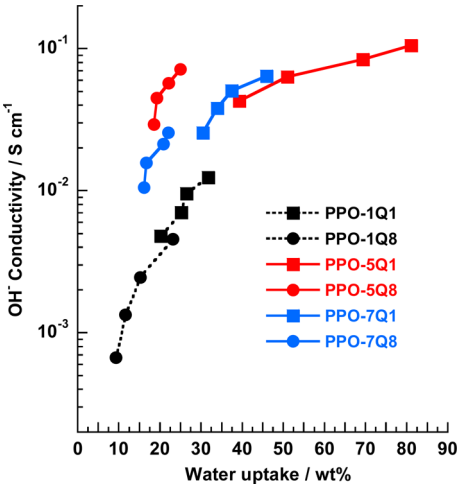

Figure 7. OH^- conductivity as a function of water uptake. Data was measured at 20, 40, 60, and 80 °C with the AEMs fully hydrated.

that the conductivity can be further enhanced by increasing the IEC without causing excessive water uptake.

Thermal and Alkaline Stability. The thermal decomposition temperature ($T_{d,95}$) of all the QA functional AEMs in the Br^- form was evaluated by TGA under N_2 at a heating rate of 10 °C min^{-1} (Figure 8). All the AEMs were found to

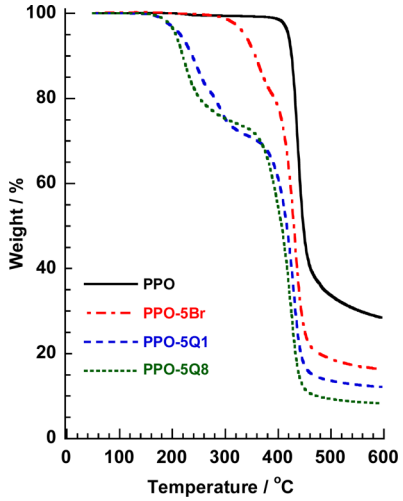

Figure 8. TGA traces of native PPO, a bromoalkylated precursor PPO (PPO-5Br-22), and quaternized samples with only a spacer unit (PPO-5Q1), and with both a spacer and an extender chain (PPO-5Q8). Samples measured under N_2 at 10 °C min^{-1}.

decompose in two steps, however at different temperatures (Table 2, Supporting Information, Figure S3). Membrane PPO-1Q1, without spacer and extender, started to decompose at $T_{d,95}$ = 199 °C, while the weight loss of the corresponding AEM with an extender chain (PPO-1Q8) began 11 °C lower, at $T_{d,95}$ = 188 °C. The AEMs with QA groups on spacer units showed higher decomposition temperatures, and the values recorded for the two membranes with only spacer units were both very close to $T_{d,95}$ ~ 213 °C, which was 14 °C higher than for PPO-1Q1. After adding an extender chain, the value of $T_{d,95}$ was found to decrease to ~206 °C. In conclusion, the addition of a spacer between the polymer backbone and QA group increased the thermal stability, while the addition of an extender seemed to decrease the stability somewhat. In any case, the thermal decomposition temperatures were all well above the typical operating temperatures of most electrochemical energy systems.

Long-term stability of AEMs under strongly alkaline conditions is of paramount importance for fuel cell applications. The basic and nucleophilic OH^- ions are known to efficiently attack both QA groups and polymer backbones, especially when the QA groups are placed in benzylic positions.[23] For example, the degradation of quaternized poly(arylene ether sulfone) backbones by chain scission has been reported to occur under quite mild condition, induced by the strong electron-withdrawing effect of the sulfone bridges and the QA groups.[43]

The evaluation of the alkaline stability of the current AEMs was performed by immersing the membranes in 1 M aq. NaOH at 80 °C. Samples were extracted after 4 and 8 days, ion exchanged to the Br^- form, and dissolved in DMSO-*d*6 before analysis by ^1H NMR spectroscopy to study possible polymer structure degradation. Figure 9 shows the spectra collected during the evaluation of PPO-1Q1, PPO-5Q1, and PPO-5Q8. For the former sample the intensity of the signal of the QA methyl protons at 3.0 ppm (I_{QA}) was found to decrease over time in relation to the intensity of the aromatic signal at 6.3–6.7 ppm (I_{Ar}), indicating a gradual degradation of the QA groups in the benzylic positions. This is in accordance with our previous results.[28] In contrast, the value of I_{QA} remained unchanged in relation with that of I_{Ar} for both PPO-5Q1 and PPO-5Q8, within the error of the NMR method. This demonstrated an excellent stability in the highly alkaline solution at 80 °C.

Figure 10 shows the evolution of I_{QA}:I_{Ar} over time in relation to the original ratio $(I_{QA}:I_{Ar})_0$ for all six AEMs. As seen, no significant change in the ratio I_{QA}:I_{Ar} was recorded for any of the AEMs based on polymers carrying QA groups via spacer units, regardless of the length of the spacer (n = 5 or 7) or the presence of an extender chain. The rationale for the exceptional stability of these AEMs may be an inherently higher stability of tetraalkylammonium in comparison to benzyltrialkylammonium, the absence of any electron-withdrawing groups directly on the backbone, and also that the spacer units allowed the formation of hydrophilic phase domains with well-hydrated OH^- ions distinctly separated from the PPO backbones. It has also been suggested that the high electron density around the β-hydrogens in long alkyl chains can inhibit Hofmann elimination reactions.[26] Pivovar and co-workers used density functional theory calculations to investigate the degradation pathways of different alkyltrimethylammonium cations.[44] They identified Hofmann elimination as the most harmful pathway, but found that the barrier toward degradation increased dramatically as the length of the alkyl chain was extended from 2 to 4 carbons because of steric interference. The present findings are in agreement with our previous results on PPO AEMs,[28] as well as with findings on low-molecular weight analogues.[24] In contrast, the I_{QA}: I_{Ar} ratio decreased gradually for both the PPO-1Q1 and PPO-1Q8 AEMs. However, the degradation rate of the AEM based on PPO-1Q8 was retarded in relation to that of PPO-1Q1, which may be due to sterical shielding of the QA groups by the long alkyl extender chain and/or the lower water uptake of the former membrane. Previously, Li et al. have reported on an enhanced stability of polymers with QA having alkyl extender chains in relation to corresponding polymers without these chains.[38] The present results clearly demonstrated the

DOI: 10.1021/acs.macromol.5b01302
Macromolecules 2015, 48, 5742–5751

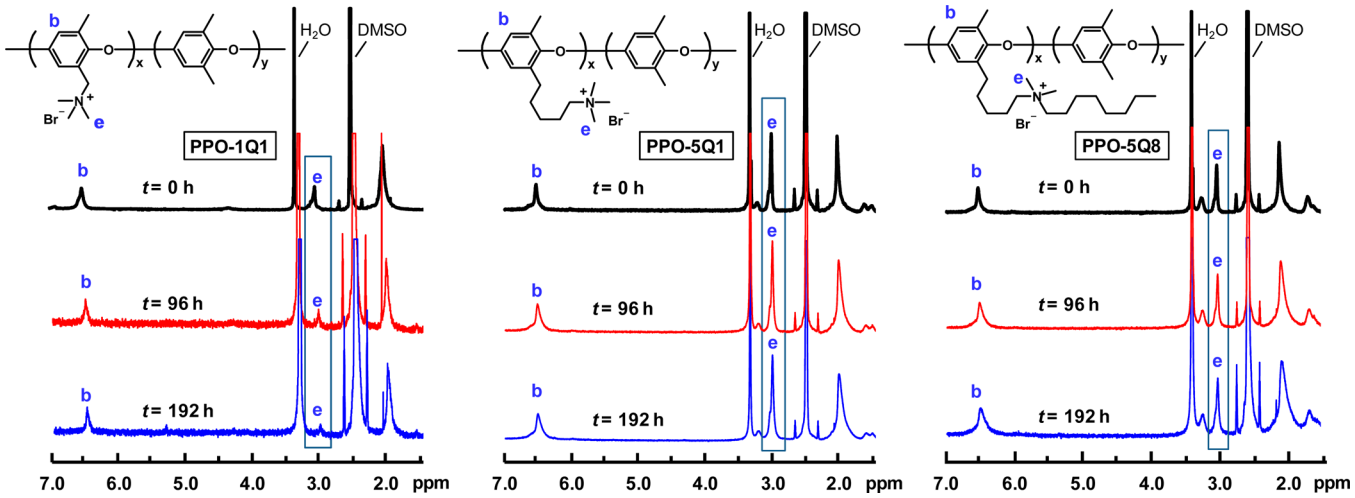

Figure 9. ^{1}H NMR spectra of PPO-1Q1, PPO-5Q1, and PPO-5Q8 stored in 1 M aqueous NaOH solution at 80 °C during 0, 96, and 192 h, respectively.

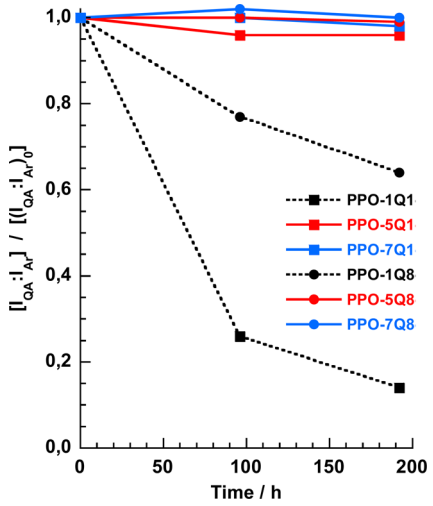

Figure 10. Evolution of the ^{1}H NMR signal ratio of the QA protons and the aromatic protons $[I_{QA}:I_{Ar}]$ during immersion in 1 M NaOH at 80 °C, in comparison with the original ratio $[(I_{QA}:I_{Ar})_0]$.

superior alkaline stability of AEMs based on polymers designed with the flexible spacer concept compared to polymers conventionally functionalized with QA groups directly on the backbone.

The performance of the present AEMs configured with spacer units alone, or with both spacer and extender chains, may be compared with that reported by Zhuang et al. of membranes based on polysulfones carrying long alkyl side chains in addition to QA groups placed directly on the backbone.[45] The phase-separated AEMs reached OH^- conductivity of 0.035 S cm^{-1} at 20 °C and above 0.1 S cm^{-1} at 80 °C. Unfortunately, these materials were found to degrade to some degree in 1 M aq. KOH at 60 °C. Zhuang and co-workers also functionalized polysulfone with side chains containing two QA groups.[46] These membranes reached 0.08 S cm^{-1} (fully hydrated at 80 °C, IEC = 2.1 mequiv g^{-1}), but degradation was noted in 3 M aq. KOH at 60 °C. Bai et al. functionalized PPO with aromatic side chains bearing three benzylic QA groups.[47] These AEMs reached an OH^- conductivity of 0.072 S cm^{-1} (fully hydrated at 60 °C, IEC = 1.5 mequiv g^{-1}), and were reported to maintain acceptable properties after 12 days in 1 M NaOH at 80 °C. Binder and co-workers attached benzylic QA groups containing a long alkyl extender chains to PPO backbones, producing AEMs quite similar to PPO-1Q8 of the present study.[48] Conductivities of 0.035 S cm^{-1} were achieved when the AEMs were fully hydrated at room temperature (IEC = 1.9 mequiv g^{-1}). Similarly to the results of the present study, these materials were found to degrade during immersion in 1 M aqueous NaOH at 80 °C. In comparison, the PPO-5Q1 and PPO-5Q8 membranes of the current work combine a OH^- conductivity of 0.11 and 0.07 S cm^{-1}, respectively at 80 °C (fully hydrated, IEC ∼ 1.5 mequiv g^{-1}) with no detectable degradation in 1 M NaOH at 80 °C during 196 h.

4. CONCLUSIONS

We have successfully synthesized PPOs tethered with flexible cationic alkyl side chains with different combinations of spacer units and extender chains by utilizing bromoalkylation and quaternization reactions. This synthetic strategy provides good control of the IEC and opportunities to attach side chains with "in-chain" and "on-chain-end" positions of the QA group. The cationic polymers were soluble in low-boiling solvents such as methanol which opens up possibilities to prepare fuel cell catalyst layers. Placing the QA groups on flexible spacer units tethered to the polymer backbone seemingly induced a high local cationic mobility which facilitated the phase separation and ionic clustering during membrane formation. This served to concentrate the ions in the AEM, as indicated by the SAXS results, which favored the development of well-hydrated and percolating OH^- ion conducting phase domains. This in turn resulted in flexible and mechanically tough AEMs with OH^- conductivities in excess of 0.1 S cm^{-1} at 80 °C. An optimum conductivity and water uptake was found between n = 1 and 5 carbon atoms in the spacer unit, implying that long alkyl spacers will increase the hydrophobicity of the AEM. All materials where the QA groups were attached via spacers also showed an excellent alkaline stability at 80 °C, while AEMs with benzylic QA groups were found to degrade over time. Constructing side chains with both spacer units and octyl extender chains on the QA groups significantly decreased the water uptake while still reaching high conductivities. Consequently, the spacer units of these materials ensured efficient

DOI: 10.1021/acs.macromol.5b01302
Macromolecules 2015, 48, 5742−5751

ionic clustering and high alkaline stability, while the addition of an extender chain facilitated high OH^- conductivity at moderate water contents. The combined results of the present study showed that AEMs with an excellent combination of chemical stability, water uptake and OH^- conductivity can be achieved by tuning the configuration of flexible cationic alkyl side chains. This provides an efficient synthetic strategy toward high-performance AEMs for alkaline fuel cell applications.

■ ASSOCIATED CONTENT

Supporting Information

The Supporting Information is available free of charge on the ACS Publications website at DOI: 10.1021/acs.macromol.5b01302.

Additional ^{1}H NMR spectra, DSC and TGA traces, and AEM solubility data (PDF)

■ AUTHOR INFORMATION

Corresponding Author

*(P.J.) E-mail: patric.jannasch@chem.lu.se.

Notes

The authors declare no competing financial interests.

■ ACKNOWLEDGMENTS

We thank the Swedish Energy Agency for financial support. We are also grateful to Annika Weiber and Marc Obiols-Rabasa for assistance with SAXS measurements and data treatment.

■ REFERENCES

(1) Varcoe, J. R.; Atanassov, P.; Dekel, D. R.; Herring, A. M.; Hickner, M. A.; Kohl, P. A.; Kucernak, A. R.; Mustain, W. E.; Nijmeijer, K.; Scott, K.; Xu, T. W.; Zhuang, L. *Energy Environ. Sci.* **2014**, *7*, 3135.
(2) Li, N. W.; Guiver, M. D. *Macromolecules* **2014**, *47*, 2175.
(3) Hickner, M. A.; Herring, A. M.; Coughlin, E. B. *J. Polym. Sci., Part B: Polym. Phys.* **2013**, *51*, 1727.
(4) Couture, G.; Alaaeddine, A.; Boschet, F.; Ameduri, B. *Prog. Polym. Sci.* **2011**, *36*, 1521.
(5) Merle, G.; Wessling, M.; Nijmeijer, K. *J. Membr. Sci.* **2011**, *377*, 1.
(6) Wang, Y. J.; Qiao, J. L.; Baker, R.; Zhang, J. J. *Chem. Soc. Rev.* **2013**, *42*, 5768.
(7) Vogel, C.; Meier-Haack, J. *Desalination* **2014**, *342*, 156.
(8) Xu, T.; Zha, F. F. *J. Membr. Sci.* **2002**, *199*, 203.
(9) Xu, T.; Yang, W. *J. Membr. Sci.* **2001**, *190*, 159.
(10) Hibbs, M. R.; Cornelius, C. *Polym. Prepr.* **2007**, *48*, 198.
(11) Yan, J. L.; Hickner, M. A. *Macromolecules* **2010**, *43*, 2349.
(12) Chen, D. Y.; Hickner, M. A. *Macromolecules* **2013**, *46*, 9270.
(13) Weiber, E. A.; Jannasch, P. *ChemSusChem* **2014**, *7*, 2621.
(14) Chen, D. Y.; Hickner, M. A. *Macromolecules* **2013**, *46*, 9270.
(15) Tanaka, M.; Fukasawa, K.; Nishino, E.; Yamaguchi, S.; Yamada, K.; Tanaka, H.; Bae, B.; Miyatake, K.; Watanabe, M. *J. Am. Chem. Soc.* **2011**, *133*, 10646.
(16) Li, X. H.; Yu, Y. F.; Liu, Q. F.; Meng, Y. Z. *J. Membr. Sci.* **2013**, *436*, 202.
(17) Jasti, A.; Shahi, V. K. *J. Power Sources* **2014**, *267*, 714.
(18) Li, Q.; Liu, L.; Miao, Q. Q.; Jin, B. K.; Bai, R. K. *Polym. Chem.* **2014**, *5*, 2208.
(19) Park, D. Y.; Kohl, P. A.; Beckham, H. W. *J. Phys. Chem. C* **2013**, *117*, 15468.
(20) Weiber, E. A.; Meis, D.; Jannasch, P. *Polym. Chem.* **2015**, *6*, 1986.
(21) Li, Q.; Liu, L.; Miao, Q. Q.; Jin, B. K.; Bai, R. K. *Chem. Commun.* **2014**, *50*, 2791.
(22) Marino, M. G.; Melchior, J. P.; Wohlfarth, A.; Kreuer, K. D. *J. Membr. Sci.* **2014**, *464*, 61.
(23) Nunez, S. A.; Hickner, M. A. *ACS Macro Lett.* **2013**, *2*, 49.
(24) Mohanty, A. D.; Bae, C. *J. Mater. Chem. A* **2014**, *2*, 17314.
(25) Marino, M. G.; Kreuer, K. D. *ChemSusChem* **2015**, *8*, 513.
(26) Tomoi, M.; Yamaguchi, K.; Ando, R.; Kantake, Y.; Aosaki, Y.; Kubota, H. *J. Appl. Polym. Sci.* **1997**, *64*, 1161.
(27) Hibbs, M. R. *J. Polym. Sci., Part B: Polym. Phys.* **2013**, *51*, 1736.
(28) Dang, H. S.; Weiber, E. A.; Jannasch, P. *J. Mater. Chem. A* **2015**, *3*, 5280.
(29) Lin, B. C.; Qiu, L. H.; Qiu, B.; Peng, Y.; Yan, F. *Macromolecules* **2011**, *44*, 9642−9649.
(30) Kulkarni, M. P.; Peckham, T. J.; Thomas, O. D.; Holdcroft, S. *MRS Online Proc. Libr.* **2014**, *1677*, 1.
(31) Xu, T.; Wu, D.; Wu, L. *Prog. Polym. Sci.* **2008**, *33*, 894.
(32) Ingratta, M.; Jutemar, E. P.; Jannasch, P. *Macromolecules* **2011**, *44*, 2074.
(33) Hsieh, H. L. *ACS Symp. Ser.* **2009**, *696*, 28.
(34) Chalk, A. J.; Hoogeboom, T. J. *J. Polym. Sci., Part A-1: Polym. Chem.* **1969**, *7*, 1359.
(35) Chalk, A. J.; Hay, A. S. *J. Polym. Sci., Part A-1: Polym. Chem.* **1969**, *7*, 691.
(36) Ingratta, M.; Elomaa, M.; Jannasch, P. *Polym. Chem.* **2010**, *1*, 739.
(37) Gebel, G.; Diat, O. *Fuel Cells* **2005**, *5*, 261.
(38) Li, N. W.; Leng, Y. J.; Hickner, M. A.; Wang, C. Y. *J. Am. Chem. Soc.* **2013**, *135*, 10124.
(39) Weiber, E. A.; Jannasch, P. *J. Membr. Sci.* **2015**, *481*, 164.
(40) Karlsson, L. E.; Jannasch, P. *J. Membr. Sci.* **2004**, *230*, 61.
(41) Lafitte, B.; Jannasch, P. *Adv. Funct. Mater.* **2007**, *17*, 2823.
(42) Jutemar, E. P.; Jannasch, P. *J. Membr. Sci.* **2010**, *351*, 87.
(43) Arges, C. G.; Ramani, V. *Proc. Natl. Acad. Sci. U. S. A.* **2013**, *110*, 2490.
(44) Long, H.; Kim, K.; Pivovar, B. S. *J. Phys. Chem. C* **2012**, *116*, 9419.
(45) Pan, J.; Chen, C.; Li, Y.; Wang, L.; Tan, L. S.; Li, G. W.; Tang, X.; Xiao, L.; Lu, J. T.; Zhuang, L. *Energy Environ. Sci.* **2014**, *7*, 354.
(46) Pan, J.; Li, Y.; Han, J. J.; Li, G. W.; Tan, L. S.; Chen, C.; Lu, J. T.; Zhuang, L. *Energy Environ. Sci.* **2013**, *6*, 2912.
(47) Li, Q.; Liu, L.; Miao, Q. Q.; Jin, B. K.; Bai, R. K. *Chem. Commun.* **2014**, *50*, 2791.
(48) Li, N. W.; Yan, T. Z.; Li, Z.; Thurn-Albrecht, T.; Binder, W. H. *Energy Environ. Sci.* **2012**, *5*, 7888.

DOI: 10.1021/acs.macromol.5b01302
Macromolecules 2015, 48, 5742−5751